This full text paper was peer reviewed at the direction of IEEE Communications Society subject matter experts for publication in the WCNC 2007 proceedings.

SIR Analysis and Interference Cancellation in Uplink OFDMA with Large Carrier Frequency and Timing Offsets

K. Raghunath and A. Chockalingam
Department of ECE, Indian Institute of Science, Bangalore 560012, INDIA

***Abstract*— In uplink OFDMA, carrier frequency offsets (CFO) and/or timing offsets (TO) of other users with respect to a desired user can cause multiuser interference (MUI). In practical uplink OFDMA systems (e.g., IEEE 802.16e standard), effect of this MUI is made acceptably small by requiring that frequency/timing alignment be achieved at the receiver with high precision (e.g., CFO must be within 1% of the subcarrier spacing and TO must be within 1/8th of the cyclic prefix duration in IEEE 802.16e), which is realized using complex closed-loop frequency/timing correction between the transmitter and the receiver. An alternate open-loop approach to handle the MUI induced by large CFOs and TOs is to employ interference cancellation techniques at the receiver. In this paper, we first analytically characterize the degradation in the average output signal-to-interference ratio (SIR) due to the combined effect of large CFOs and TOs in uplink OFDMA. We then propose a parallel interference canceller (PIC) for the mitigation of interference due to CFOs and TOs in this system. We show that the proposed PIC effectively mitigates the performance loss due to CFO/TO induced interference in uplink OFDMA.**

Keywords *– Uplink OFDMA, carrier frequency offset, timing offset, imperfect synchronization, multiuser interference, interference cancellation.*

I. Introduction

Recent research has been witnessing increased focus on orthogonal frequency division multiple access (OFDMA) on the uplink [1]-[8]. Practical systems like IEEE 802.16e standard use OFDMA on the uplink [9]. The performance of uplink OFDMA systems depend to a large extent on how well the orthogonality among different subcarriers is maintained at the receiver. Factors including carrier frequency offsets (CFO) of different users induced by Doppler effects and/or poor oscillator alignments, and timing offsets (TO) of different users caused by timing misalignment due to imperfect synchronization and path delay differences between different users can destroy the orthogonality among different subcarriers and cause multiuser interference (MUI).

In order to avoid the detrimental effect of the CFO-induced MUI, practical systems often mandate that carrier frequency alignment be achieved at the receiver with high accuracy (e.g., IEEE 802.16e standard requires that the CFO be brought within 1% of the subcarrier spacing [9]). Such high precision frequency alignment is often realized using complex closed-loop frequency correction between the transmitter and the receiver, which requires feedback bandwidth.

The TOs of other users in uplink OFDMA depend on the magnitude of the difference in path delays between the desired user and the other users. A large cell radius would imply large TOs. The detrimental effect of TO-induced orthogonality loss can be alleviated by i) providing adequate guard time (expensive in terms of throughput for large TOs), or ii) use of GPS timing (expensive in terms of hardware at the user terminals), or iii) closed-loop timing correction techniques (expensive in terms of feedback bandwidth). IEEE 802.16e standard, for example, mandates that the TO be brought within 1/8th of the cyclic prefix duration [9], and this necessitates the use of closed-loop timing correction approach.

An alternate open-loop approach to handle the effects of large CFOs and TOs in uplink OFDMA is to employ interference cancelling (IC) receivers at the base station. An ability to handle large CFOs and TOs using IC techniques can allow low-cost transmit oscillators to be used at all user terminals in an open-loop mode, which can reduce cost and complexity. Receivers employing the IC approach to handle the effects of CFOs alone, assuming ideal time synchronization and sampling (in other words, assuming no orthogonality loss due to timing offsets) have been proposed in [6],[7],[8]. Several papers have reported the effect of TOs on OFDM/OFDMA performance [10]-[13]. These papers, however, are not concerned with cancellation of interference caused by TOs in uplink OFDMA when TOs are larger than the cyclic prefix. To our knowledge, cancellation of interference caused by both CFOs as well as TOs has not been reported so far. In this paper, we first analytically characterize the degradation of signal-to-interference ratio (SIR) at the DFT output of the receiver as a function of CFOs and TOs in uplink OFDMA. In [11],[12] SIR expressions are derived for the case of TO only, whereas in [13] CFO and TO are considered but only for OFDM (not for multiuser uplink OFDMA). In addition to our SIR analysis, we propose a parallel interference canceller (PIC) for mitigation of interference due to CFOs and TOs in this system. We evaluate the bit error performance of the PIC through simulations and show that the PIC effectively mitigates the performance loss due to CFO/TO-induced interference in uplink OFDMA.

The rest of the paper is organized as follows. In Sec. II, we present the system model. The SIR analysis and results are presented in Sec. III. The PIC receiver for this system and its BER performance are presented in Sec. IV. Conclusions are given in Sec. V.

II. System Model

We consider an uplink OFDMA system with K users, where each user communicates with a base station through an independent multipath channel. We assume that there are N subcarriers in each OFDM symbol and one subcarrier can be allocated to only one user. The information symbol for

This work was supported in part by the DRDO-IISc Program on Advanced Research in Mathematical Engineering.

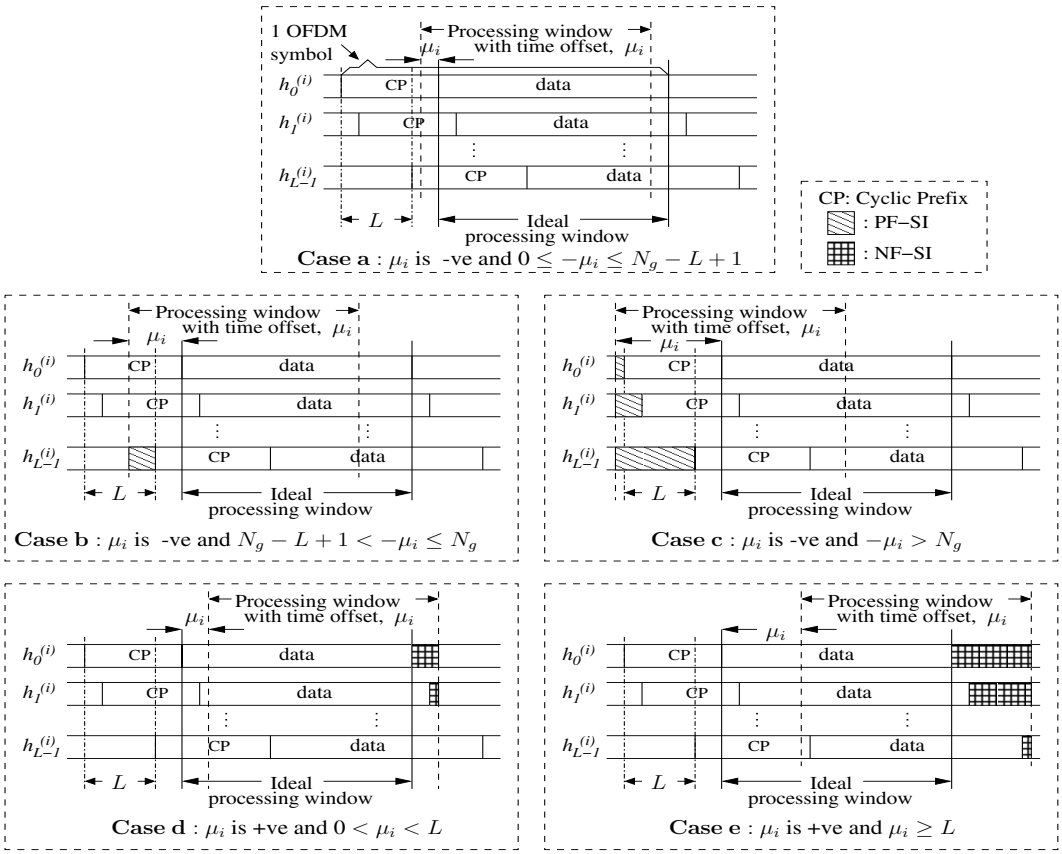

Fig. 1. Different timing misalignment scenarios in single user OFDM. Only self interferences.

the ith user on the kth subcarrier is denoted by $X_k^{(i)}$, $k \in S_i$, where S_i is the set of subcarriers assigned to user i and $E\Big[\Big|X_k^{(i)}\Big|^2\Big] = 1$. Then, $\bigcup_{i=1}^{K} S_i = \{0, 1, \ldots, N-1\}$ and $S_i \bigcap S_j = \phi$, for $i \neq j$. The length of the cyclic prefix added is N_g sampling periods[1], and is assumed to be longer than the maximum channel delay spread normalized by the sampling period, L, (i.e., $N_g > L$). After IDFT processing and cyclic prefix insertion at the transmitter, the time-domain sequence of the ith user, $x_n^{(i)}$, is given by

$$x_n^{(i)} = \frac{1}{N} \sum_{k \in S_i} X_k^{(i)} e^{\frac{j2\pi nk}{N}}, \quad -N_g \le n \le N-1. \quad (1)$$

The ith user's signal at the receiver input, after passing through the channel, is given by

$$s_n^{(i)} = x_n^{(i)} \star h_n^{(i)}, \quad (2)$$

where $\star$ denotes linear convolution and $h_n^{(i)}$ is the ith user's channel impulse response. It is assumed that $h_n^{(i)}$ is non-zero only for $n = 0, \ldots, L-1$, and that all users' channels are statistically independent. We assume that $h_n^{(i)}$'s are i.i.d. complex Gaussian with zero mean and $E\Big[\Big(h_{n,I}^{(i)}\Big)^2\Big] = E\Big[\Big(h_{n,Q}^{(i)}\Big)^2\Big] = 1/2L$, where $h_{n,I}^{(i)}$ and $h_{n,Q}^{(i)}$ are the real and imaginary parts of $h_n^{(i)}$. The channel coefficient in frequency-domain $H_k^{(i)}$ is given by

$$H_k^{(i)} = \sum_{n=0}^{L-1} h_n^{(i)} e^{\frac{-j2\pi nk}{N}} \quad \text{and} \quad E\Big[\Big|H_k^{(i)}\Big|^2\Big] = 1. \quad (3)$$

Let $\epsilon_i, i = 1, 2, \cdots, K$ denote ith user's residual CFO normalized by the subcarrier spacing, and $\mu_i, i = 1, 2, \cdots, K$ denote ith user's residual TO in number of sampling periods at the receiver. The timing offsets μ_i's can be positive ($\mu_i > 0$) or negative ($\mu_i < 0$).

A. Cases of Timing Misalignment for $\mu_i < 0$ and $\mu_i > 0$

Consider the case of TOs only (i.e., $\epsilon_i = 0, \forall i$). For $\mu_i < 0$, depending on the magnitude of μ_i compared to delay spread L and cyclic prefix duration N_g, interference from previous frame data (which we refer to as *Previous Frame Self Interference* (PF-SI)) and inter-carrier interference due to loss of some samples of the current frame in the processing window (which we refer to as *Current Frame Self Interference* (CF-SI)) may or may not occur. We need to consider the following three cases for $\mu_i < 0$.

- **Case a):** $0 \le -\mu_i \le N_g - L + 1$, where there will be no loss of orthogonality, and hence there is no interference.
- **Case b):** $N_g - L + 1 < -\mu_i \le N_g$, where PF-SI is caused by some paths. The number of such paths causing PF-SI in this case will be $L - [(N_g + \mu_i) + 1]$. In addition, since up to $L - [(N_g + \mu_i) + 1]$ samples of the current frame are lost in the processing window, it results in loss of orthogonality and hence in CF-SI.
- **Case c):** $-\mu_i > N_g$, where PF-SI is caused by all the L paths. In addition, CF-SI also occurs due to loss of up to L samples of the current frame.

[1]Let T denote one OFDM symbol period including the cyclic prefix duration. Then $T_s = \frac{T}{N+N_g}$ denotes one sampling period.

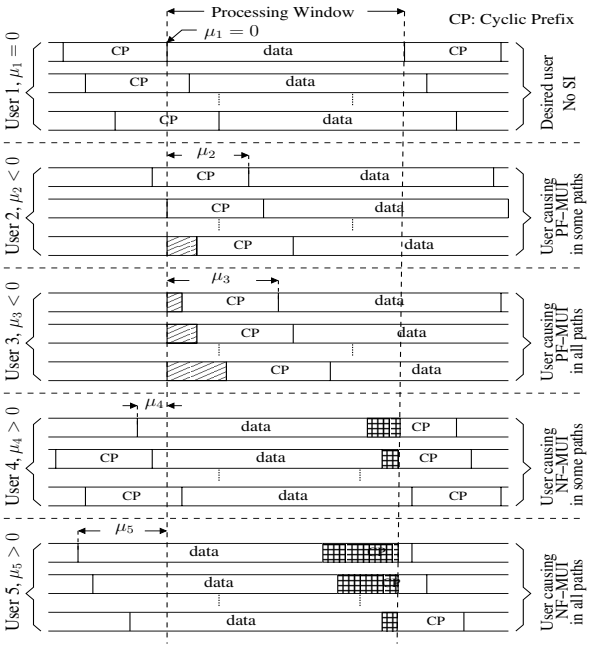

Fig. 2. Different timing misalignment scenarios in multiuser scenario.

For $\mu_i > 0$, any value of $\mu_i > 0$ will cause both interference from next frame data (which we refer to as *Next Frame Self Interference* (NF-SI) as well as CF-SI due to loss of some samples in the current frame. The following two cases need to be considered for $\mu_i > 0$.

- **Case d):** $0 < \mu_i < L$, where NF-SI is caused by some paths. The number of such paths causing NF-SI in this case is $L - \mu_i$. In addition, CF-SI also will occur due to loss of up to μ_i samples in the current frame.
- **Case e):** $\mu_i \geq L$, where NF-SI is caused by all paths. CF-SI will occur in this case as well.

In Fig. 1, we illustrate the timing misalignment scenarios for the above five cases a) to e) for a given user i in the absence of other users, in which case the interferences are essentially self interferences. In addition to the above self interferences, other user interference will occur in the multiuser case. In the multiuser case also, the same five cases apply, and the corresponding multiuser interference (MUI) terms caused by previous, current and next frame data symbols of other users are denoted by *Previous Frame MUI* (PF-MUI), *Current Frame MUI* (CF-MUI), and *Next Frame MUI* (NF-MUI), respectively. In Fig. 2, we illustrate a possible time misalignment scenario for the multiuser case where the desired user is perfectly aligned (i.e., no self interferences) and the other users are misaligned (causing PF-MUI, CF-MUI, NF-MUI).

In the presence of both TOs as well as CFOs, additional CFO-induced interference will be generated. When there is no TO-induced interference on a given path, we refer to the interference generated by the desired user CFO as *CFO-induced Self Interference* (CFO-SI) on that path, and those generated by the other user CFOs as *CFO-induced MUI* (CFO-MUI) on that path. On all the paths that experience TO-induced interferences, non-zero CFOs (i.e., ϵ_i's) will affect PF-SI/MUI, CF-SI/MUI and NF-SI/MUI.

III. SIR Analysis

In this section, we present the received signal expressions at the output of the DFT for the various TO cases a) to e) in the presence of CFOs, and obtain expressions for the output SIR.

Case a): $\mu_i < 0$, $0 \leq -\mu_i \leq N_g - L + 1$, and $\epsilon_i > 0$: In this case, there is no TO-induced interference on all paths of all users, but there is CFO-induced interference (i.e., CFO-SI/MUI). The output of the DFT block of the desired user d on the kth subcarrier, $Y_k^{(d)}$, due to signals from all the users over all the paths can be derived as

$$Y_k^{(d)} = \underbrace{X_k^{(d)} e^{\frac{j2\pi\mu_d k}{N}} \sum_{l=0}^{L-1} h_l^{(d)} e^{\frac{-j2\pi lk}{N}} \Gamma_{kk}^{(d)}}_{\text{Desired signal}} + \underbrace{\sum_{\substack{q\in S_d \\ q\neq k}} X_q^{(d)} e^{\frac{j2\pi\mu_d q}{N}} \sum_{l=0}^{L-1} h_l^{(d)} e^{\frac{-j2\pi lq}{N}} \Gamma_{qk}^{(d)}}_{\text{CFO-SI}} + \underbrace{\sum_{q\in S_j, j\neq d} X_q^{(j)} e^{\frac{j2\pi\mu_j q}{N}} \sum_{l=0}^{L-1} h_l^{(j)} e^{\frac{-j2\pi lq}{N}} \Gamma_{qk}^{(j)}}_{\text{CFO-MUI}} + Z_k^{(d)}, \quad (4)$$

where

$$\Gamma_{qk}^{(i)} = \frac{1}{N} \sum_{n=0}^{N-1} e^{\frac{j2\pi n(q+\epsilon_i - k)}{N}}. \quad (5)$$

Case b) $\mu_i < 0$, $N_g - L + 1 < -\mu_i \leq N_g$, and $\epsilon_i > 0$: Since some of the paths do not experience TO-induced interference and the remaining paths experience interference from previous frame in this case, there will be PF-SI/MUI, CF-SI/MUI, and CFO-SI/MUI. The DFT output of the desired user d on the kth subcarrier in this case can be derived as

$$Y_k^{(d)} = \underbrace{X_k^{(d)} e^{\frac{j2\pi\mu_d k}{N}} \sum_{l=0}^{L-1} h_l^{(d)} e^{\frac{-j2\pi lk}{N}} \Gamma_{kk}^{(d)(l)}}_{\text{Desired signal}} + \underbrace{\sum_{\substack{q\in S_d \\ q\neq k}} X_q^{(d)} e^{\frac{j2\pi\mu_d q}{N}} \sum_{l=0}^{L-1} h_l^{(d)} e^{\frac{-j2\pi lk}{N}} \Gamma_{qk}^{(d)(l)}}_{\text{CF-SI, CFO-SI}} + \underbrace{\sum_{\substack{q\in S_j \\ j\neq d}} X_q^{(j)} e^{\frac{j2\pi\mu_j q}{N}} \sum_{l=0}^{L-1} h_l^{(j)} e^{\frac{-j2\pi lq}{N}} \Gamma_{qk}^{(j)(l)}}_{\text{CF-MUI, CFO-MUI}} + \underbrace{\sum_{q\in S_d} X_q^{(d)(p)} e^{\frac{j2\pi(\mu_d+N_g)q}{N}} \sum_{l=N_g+\mu_d+1}^{L-1} h_l^{(d)} e^{\frac{-j2\pi lq}{N}} \rho_{qk}^{(d)(l)}}_{\text{PF-SI}} + \underbrace{\sum_{\substack{q\in S_j \\ j\neq d}} X_q^{(j)(p)} e^{\frac{j2\pi(\mu_d+N_g)q}{N}} \sum_{l=N_g+\mu_d+1}^{L-1} h_l^{(j)} e^{\frac{-j2\pi lq}{N}} \rho_{qk}^{(j)(l)}}_{\text{PF-MUI}} + Z_k^{(d)}, \quad (6)$$

where $X_q^{(j)(p)}$ is the previous frame data symbol of the jth user on the qth subcarrier, and $\Gamma_{qk}^{(i)(l)}$ is given by (5) and $\rho_{qk}^{(i),(l)} = 0$ for $0 < l \leq N_g + \mu_i$. For $l > N_g + \mu_i$, $\Gamma_{qk}^{(i)(l)}$ and $\rho_{qk}^{(i)(l)}$ are given by

$$\Gamma_{qk}^{(i)(l)} = \frac{1}{N}\sum_{n=-\mu_i-N_g+l}^{N-1} e^{\frac{j2\pi n(q+\epsilon_i-k)}{N}}, \quad (7)$$

$$\rho_{qk}^{(i)(l)} = \frac{1}{N}\sum_{n=0}^{-\mu_i-N_g-1+l} e^{\frac{j2\pi n(q+\epsilon_i-k)}{N}}. \quad (8)$$

Case c): $\mu_i < 0$, $-\mu_i > N_g$, and $\epsilon_i > 0$: Since all paths experience interference from previous frame in this case, there will be PF-SI/MUI and CF-SI/MUI. The DFT output of the desired user d on the kth subcarrier in this case is derived as

$$\begin{aligned} Y_k^{(d)} = & \underbrace{X_k^{(d)} e^{\frac{j2\pi\mu_d k}{N}} \sum_{l=0}^{L-1} h_l^{(d)} e^{\frac{-j2\pi lk}{N}} \Gamma_{kk}^{(d)(l)}}_{\text{Desired signal}} \\ & + \underbrace{\sum_{\substack{q\in S_d \\ q\neq k}} X_q^{(d)} e^{\frac{j2\pi\mu_d q}{N}} \sum_{l=0}^{L-1} h_l^{(d)} e^{\frac{-j2\pi lq}{N}} \Gamma_{qk}^{(d)(l)}}_{\text{CF-SI}} \\ & + \underbrace{\sum_{q\in S_d} X_q^{(d)(p)} e^{\frac{j2\pi(\mu_d+N_g)q}{N}} \sum_{l=0}^{L-1} h_l^{(d)} e^{\frac{-j2\pi lq}{N}} \rho_{qk}^{(d)(l)}}_{\text{PF-SI}} \\ & + \underbrace{\sum_{\substack{q\in S_j \\ j\neq d}} X_q^{(j)} e^{\frac{j2\pi\mu_j q}{N}} \sum_{l=0}^{L-1} h_l^{(j)} e^{\frac{-j2\pi lq}{N}} \Gamma_{qk}^{(j)(l)}}_{\text{CF-MUI}} \\ & + \underbrace{\sum_{\substack{q\in S_j \\ j\neq d}} X_q^{(j)(p)} e^{\frac{j2\pi(\mu_d+N_g)q}{N}} \sum_{l=0}^{L-1} h_l^{(j)} e^{\frac{-j2\pi lq}{N}}}_{\text{PF-MUI}} + Z_k^{(d)}. \quad (9) \end{aligned}$$

where $\Gamma_{qk}^{(i)(l)}$ and $\rho_{qk}^{(i)(l)}$ are given by (7) and (8), respectively, and $Z_k^{(d)}$ is the noise term.

Case d): $\mu_i > 0$, $0 < \mu_i < L$, and $\epsilon_i > 0$: This case is similar to *Case b*) except that there will be interference from next frame instead of previous frame. That is, there will be NF-SI/MUI, CF-SI/MUI, and CFO-SI/MUI in this case.

Defining, for $0 \le l \le \mu_i - 1$,

$$\xi_{qk}^{(i)(l)} = \frac{1}{N}\sum_{n=N-\mu_i+l}^{N-1} e^{\frac{j2\pi n(q+\epsilon_i-k)}{N}} \quad (10)$$

$$\zeta_{qk}^{(i)(l)} = \frac{1}{N}\sum_{n=0}^{N-1-\mu_i+l} e^{\frac{j2\pi n(q+\epsilon_i-k)}{N}}, \quad (11)$$

and, for $l \ge \mu_i$,

$$\zeta_{qk}^{(i)} = \frac{1}{N}\sum_{n=0}^{N-1} e^{\frac{j2\pi n(q+\epsilon_i-k)}{N}}, \quad \text{and} \quad \xi_{qk}^{(i)(l)} = 0, \quad (12)$$

the DFT output of the desired user d on the kth subcarrier in this case can be derived as

$$\begin{aligned} Y_k^{(d)} = & \underbrace{X_k^{(d)} e^{\frac{j2\pi\mu_d k}{N}} \sum_{l=0}^{L-1} h_l^{(d)} e^{\frac{-j2\pi lk}{N}} \zeta_{kk}^{(d)(l)}}_{\text{Desired signal}} \\ & + \underbrace{\sum_{\substack{q\in S_d \\ q\neq k}} X_q^{(d)} e^{\frac{j2\pi\mu_d q}{N}} \sum_{l=0}^{L-1} h_l^{(d)} e^{\frac{-j2\pi lq}{N}} \zeta_{qk}^{(d)(l)}}_{\text{CF-SI, CFO-SI}} \\ & + \underbrace{\sum_{q\in S_d} X_q^{(d)(n)} e^{\frac{-j2\pi(N_g-\mu_d)q}{N}} \sum_{l=0}^{L-1} h_l^{(d)} e^{\frac{-j2\pi lq}{N}} \xi_{qk}^{(d)(l)}}_{\text{NF-SI}} \\ & + \underbrace{\sum_{\substack{q\in S_j \\ j\neq d}} X_q^{(j)} e^{\frac{j2\pi\mu_j q}{N}} \sum_{l=0}^{L-1} h_l^{(j)} e^{\frac{-j2\pi lq}{N}} \zeta_{qk}^{(j)(l)}}_{\text{CF-MUI, CFO-MUI}} \\ & + \underbrace{\sum_{\substack{q\in S_j \\ j\neq d}} X_q^{(j)(n)} e^{\frac{-j2\pi(N_g-\mu_j)q}{N}} \sum_{l=0}^{L-1} h_l^{(j)} e^{\frac{-j2\pi lq}{N}} \xi_{qk}^{(j)(l)}}_{\text{NF-MUI}} + Z_k^{(d)}, \quad (13) \end{aligned}$$

where $X_q^{(j)(n)}$ is the next frame data symbol of the jth user on the qth subcarrier.

Case e): $\mu_i > 0$, $\mu_i \ge L$, and $\epsilon_i > 0$: Since all paths experience interference from next frame in this case, there will be NF-SI/MUI and CF-SI/MUI. The DFT output of the desired user d on the kth subcarrier in this case is derived as

$$\begin{aligned} Y_k^{(d)} = & \underbrace{X_k^{(d)} e^{\frac{j2\pi\mu_d k}{N}} \sum_{l=0}^{L-1} h_l^{(d)} e^{\frac{-j2\pi lk}{N}} \zeta_{kk}^{(d)(l)}}_{\text{Desired signal}} \\ & + \underbrace{\sum_{\substack{q\in S_d \\ q\neq k}} X_q^{(d)} e^{\frac{j2\pi\mu_d q}{N}} \sum_{l=0}^{L-1} h_l^{(d)} e^{\frac{-j2\pi lq}{N}} \zeta_{qk}^{(d)(l)}}_{\text{CF-SI}} \\ & + \underbrace{\sum_{q\in S_d} X_q^{(d)(n)} e^{\frac{-j2\pi(N_g-\mu_d)q}{N}} \sum_{l=0}^{L-1} h_l^{(d)} e^{\frac{-j2\pi lq}{N}} \xi_{qk}^{(d)(l)}}_{\text{NF-SI}} \\ & + \underbrace{\sum_{\substack{q\in S_j \\ j\neq d}} X_q^{(j)} e^{\frac{j2\pi\mu_j q}{N}} \sum_{l=0}^{L-1} h_l^{(j)} e^{\frac{-j2\pi lq}{N}} \zeta_{qk}^{(j)(l)}}_{\text{CF-MUI}} \\ & + \underbrace{\sum_{\substack{q\in S_j \\ j\neq d}} X_q^{(j)(n)} e^{\frac{-j2\pi(N_g-\mu_j)q}{N}} \sum_{l=0}^{L-1} h_l^{(j)} e^{\frac{-j2\pi lq}{N}} \xi_{qk}^{(j)(l)}}_{\text{NF-MUI}} + Z_k^{(d)}, \quad (14) \end{aligned}$$

where $\xi_{qk}^{(i)(l)}$ and $\zeta_{qk}^{(i)(l)}$ are given by (10) and (11), respectively.

A. SIR Expressions

From the DFT output expressions in the above for the five different cases of timing misalignment, the expressions for the average SIR at the output of the DFT, with no noise, can be derived to be as follows. We denote the average output

SIR of the desired user d on the kth subcarrier for the time misalignment *Case* λ, $\lambda \in \{$a,b,c,d,e$\}$ as $\left(\overline{SIR}_k^{(d)}\right)_\lambda$, which can be written in the following form

$$\left(\overline{SIR}_k^{(d)}\right)_\lambda = \frac{A_\lambda}{B_\lambda + C_\lambda + D_\lambda + E_\lambda}. \quad (15)$$

- For the misalignment *Case a)*,

$$A_a = \sum_{l=0}^{L-1} \left|\Gamma_{kk}^{(d)(l)}\right|^2, \quad B_a = \sum_{\substack{q\in S_d \\ q\neq k}} \sum_{l=0}^{L-1} \left|\Gamma_{qk}^{(d)(l)}\right|^2,$$

$$C_a = \sum_{\substack{q\in S_j \\ j\neq d}} \sum_{l=0}^{L-1} \left|\Gamma_{qk}^{(j)(l)}\right|^2, \quad D_a = 0, \quad \text{and} \quad E_a = 0,$$

  where $\Gamma_{qk}^{(j)(l)}$ is given by (5).
- For the misalignment *Case b)*

$$A_b = \sum_{l=0}^{L-1} \left|\Gamma_{kk}^{(d)(l)}\right|^2, \quad B_b = \sum_{\substack{q\in S_d \\ q\neq k}} \sum_{l=0}^{L-1} \left|\Gamma_{qk}^{(d)(l)}\right|^2,$$

$$C_b = \sum_{\substack{q\in S_j \\ j\neq d}} \sum_{l=0}^{L-1} \left|\Gamma_{qk}^{(j)(l)}\right|^2, \quad D_b = \sum_{\substack{q\in S_d \\ q\neq k}} \sum_{l=0}^{L-1} \left|\rho_{qk}^{(d)(l)}\right|^2,$$

$$E_b = \sum_{\substack{q\in S_j \\ j\neq d}} \sum_{l=0}^{L-1} \left|\rho_{qk}^{(j)(l)}\right|^2,$$

  where $\Gamma_{qk}^{(i)(l)}$ for $0 \le l \le N_g + \mu_i$ is given by (5), and $\Gamma_{qk}^{(i)(l)}$ and $\rho_{qk}^{(i)(l)}$ for $N_g + \mu_i < l \le L-1$ are given by (7) and (8), respectively.
- For the misalignment *Case c)*, the terms in the numerator and denominator in (15) are same as that of *Case b)* in the above, except that for all l, $\Gamma_{qk}^{(i)(l)}$ and $\rho_{qk}^{(i)(l)}$ are given by (7) and (8), respectively.
- For the misalignment *Case d)*,

$$A_d = \sum_{l=0}^{L-1} \left|\zeta_{kk}^{(d)(l)}\right|^2, \quad B_d = \sum_{\substack{q\in S_d \\ q\neq k}} \sum_{l=0}^{L-1} \left|\zeta_{qk}^{(d)(l)}\right|^2,$$

$$C_d = \sum_{\substack{q\in S_j \\ j\neq d}} \sum_{l=0}^{L-1} \left|\zeta_{qk}^{(j)(l)}\right|^2, \quad D_d = \sum_{\substack{q\in S_d \\ q\neq k}} \sum_{l=0}^{L-1} \left|\xi_{qk}^{(d)(l)}\right|^2,$$

$$E_d = \sum_{\substack{q\in S_j \\ j\neq d}} \sum_{l=0}^{L-1} \left|\xi_{qk}^{(j)(l)}\right|^2,$$

  where, for $0 \le l \le \mu_i - 1$, $\xi_{qk}^{(i)(l)}$ and $\zeta_{qk}^{(i)(l)}$ are given by (10) and (11), respectively, and for $\mu_i \le l \le L-1$ they are given by (12).
- For the misalignment *Case e)*, the terms in the numerator and denominator in (15) are same as that of *Case d)* in the above, except that for all l, $\xi_{qk}^{(d)(l)}$ and $\zeta_{qk}^{(j)(l)}$ are given by (10) and (11), respectively.

B. SIR Results and Discussions

We computed the average SIR at the DFT output given by the expressions in the previous subsection and plotted them in Figs. 3 and 4. In Fig. 3, a single user with CFO ϵ, and TO μ is considered, and in Fig. 4, four users ($K = 4$) with different CFOs ϵ_i's and TOs μ_i's are considered. Other system parameters used are: $N = 64$, $L = 10$, $N_g = 12$.

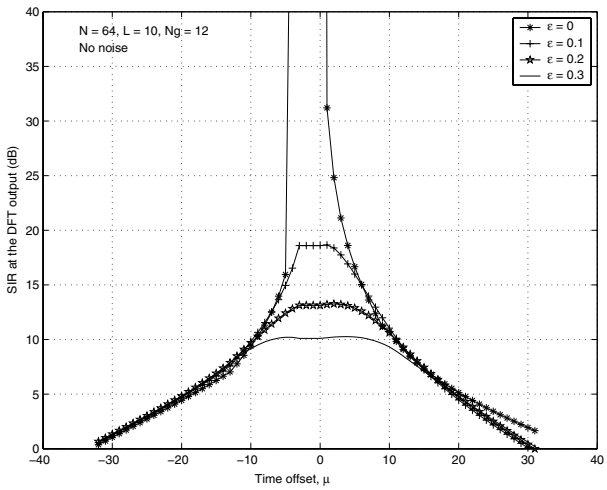

Fig. 3. SIR at the output of the DFT in single user OFDM with CFO, ϵ, and TO, μ. $N = 64$, $L = 10$, $N_g = 12$, no noise. Analytical results matched with simulation results.

Fig. 3 shows the output SIR as a function of μ for different values of $\epsilon = 0, 0.1, 0.2, 0.3$. We have verified these analytical plots using simulations also. We found the analytical results to match closely with the simulation results. In the ideal case of $\mu = \epsilon = 0$, the SIR is infinite (since no noise), and for non-zero μ and ϵ, SIR degrades due to the various self interference terms caused by CFO and TO. Note that even in the case of perfect timing alignment (i.e., $\mu = 0$), SIR degradation happens due to non-zero frequency offset ($\epsilon \neq 0$). Also, in the case of perfect frequency alignment ($\epsilon = 0$), SIR degrades due to imperfect timing alignment ($\mu \neq 0$). While the SIR starts degrading for $\mu = 1$ itself due to NF-SI in case of $\mu > 0$, there is no SIR degradation due to negative time offset up to $-(N_g - L + 1)$ (i.e., up to $\mu = -3$ in this example) since PF-SI gets introduced only for $\mu < -(N_g - L + 1)$. In Fig. 4, we plot the SIR degradation due to multiuser interference caused due to other user signals. Here, we take the desired user 1 to be perfectly aligned in time and frequency (i.e., $\mu_1 = \epsilon_1 = 0$), and the remaining three users to have the same offsets (i.e., $\epsilon_2 = \epsilon_3 = \epsilon_4$ and $\mu_2 = \mu_3 = \mu_4$). It can be seen that there is significant loss in output SIR in the multiuser case because of the additional MUI terms generated. We further observe that this SIR degradation due to CFOs and TOs can be alleviated using interference cancellation techniques, an example of which is illustrated in the following section.

IV. PIC Receiver

The large CFO/TO received signal model employed in the analysis of the previous section can be used in the cancellation of the CFO- and TO-induced interferences. In particular, multistage PIC receivers can be devised using estimates of the present and previous data symbols of the desired as well as the other users.

Figure 5 shows the proposed PIC receiver for cancelling the CFO- and TO-induced interferences. The receiver first performs CFO compensation (by multiplying the received signal with $\exp(-j2\pi\hat{\epsilon}_i n/N)$, where $\hat{\epsilon}_i$ is an estimate of ϵ_i, followed by DFT operation and multistage interference cancel-

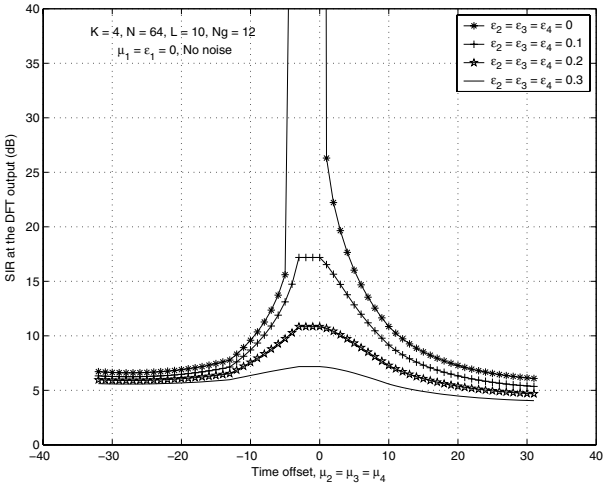

Fig. 4. SIR at the output of the DFT in multiuser uplink OFDMA with CFOs and TOs. $K = 4$, $N = 64$, $L = 10$, $N_g = 12$, block allocation of subcarriers, $\epsilon_1 = \mu_1 = 0$, $\epsilon_2 = \epsilon_3 = \epsilon_4$, $\mu_2 = \mu_3 = \mu_4$, no noise. Analytical results matched with simulation results.

lation. Estimates of the current and previous data symbols on all subcarriers at the DFT output ($\widehat{X}_k^{(i)}$'s and $\widehat{X}_k^{(i)(p)}$'s) are made, which, along with the estimates of the channel coefficients, are then used to reconstruct the interference terms. The reconstructed interference terms are then subtracted from the received signal. These steps are repeated in multiple stages of cancellation.

In Fig. 6, we present the BER performance of the 2nd and 3rd stages of the PIC receiver in an uplink OFDMA system with $K = 4$, $N = 16$, block allocation of equal-power subcarriers, $L = 2$, $N_g = 4$, and BPSK modulation. The TOs and CFOs considered are $[\mu_1, \mu_2, \mu_3, \mu_4] = [-6, -8, -10, -12]$ and $[\epsilon_1, \epsilon_2, \epsilon_3, \epsilon_4] = [-0.1, 0.3, 0.25, -0.15]$. We assume perfect estimates of ϵ_i's, μ_i's, and channel coefficients in the simulations. The performance of the MF detector (no cancellation) as well as no interference performance are also plotted for comparison. It can be observed that the PIC receiver effectively cancels the CFO- and TO-induced interferences.

V. Conclusions

We analytically characterized the degradation in the average output SIR due to large CFOs and TOs in uplink OFDMA. We presented a PIC receiver that effectively cancelled the interferences caused by CFOs and TOs. The proposed PIC approach to handle CFOs and TOs in uplink OFDMA can allow the use of low-cost transmit oscillators in all user terminals in an open-loop mode, which in turn can reduce user terminal cost and complexity.

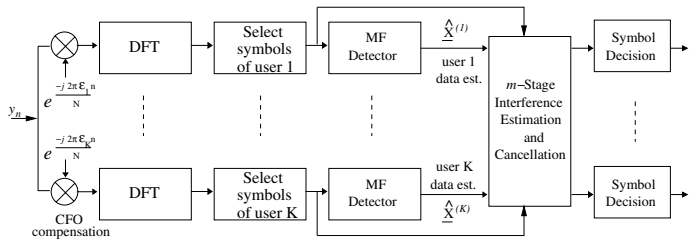

Fig. 5. PIC receiver for cancellation of interferences due to CFOs and TOs in uplink OFDMA.

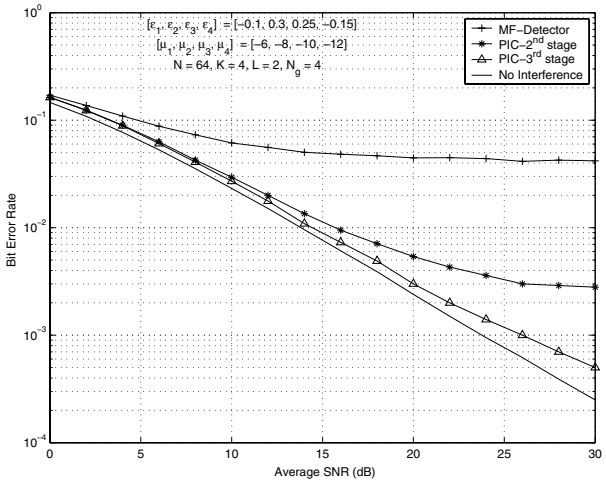

Fig. 6. BER performance of the proposed PIC receiver. $K = 4$, $N = 64$, $L = 2$, $N_g = 4$. $[\epsilon_1, \epsilon_2, \epsilon_3, \epsilon_4] = [-0.1, 0.3, 0.25, -0.15]$, $[\mu_1, \mu_2, \mu_3, \mu_4] = [-6, -8, -10, -12]$, block allocation, BPSK modulation.

References

[1] Z. R. Cao, U. Tureli, and Y-D. Yao, "Deterministic multiuser carrier frequency offset estimation for interleaved OFDMA uplink," *IEEE Trans. on Commun.,* vol. 52, no. 9, pp. 1585-1594, 2004.

[2] H. Wang and B. Chen, "Asymptotic distributions and peak power analysis for uplink OFDMA," *Proc. IEEE ICASSP'2004*, May 2004.

[3] M. O. Pun, C.-C. J. Juo, and M. Morelli, "Joint synchronization and channel estimation in uplink OFDMA systems," *Proc. IEEE ICASSP'2005*, March 2005.

[4] J. Choi, C. Lee, H. W. Jung, and Y. H. Lee, "Carrier frequency offset compensation for uplink of OFDM-FDMA systems," *IEEE Commun. Letters*, vol. 4, no. 12, pp. 414-416, December 2000.

[5] Z. Cao, U. Tureh, and Y. D. Yao, "Analysis of two receiver schemes for interleaved OFDMA uplink signals," *36th Asilomar Conf. on Signals, Systems & Computers,* vol. 2, pp. 1818-1821, November 2002.

[6] R. Fantacci, D. Marabissi, and S. Papini, "Multiuser interference cancellation receivers for OFDMA uplink communications with carrier frequency offset," *Proc. IEEE GLOBECOM'04*, pp. 2808-2812, 2004.

[7] D. Huang and K. B. Letaief, "An interference cancellation scheme for carrier frequency offsets correction in OFDMA systems," *IEEE Trans. on Commun.,* vol. 53, no. 7, pp. 1155-1165, July 2005.

[8] S. Manohar, V. Tikiya, D. Sreedhar, and A. Chockalingam, "A multiuser interference cancellation scheme for uplink OFDMA," *Proc. IEEE WCNC'2006*, April 2006. Also to appear in *IEEE Trans. on Wireless Commun.*

[9] IEEE 802.16e-2005: IEEE standard for Local and Metropolitan Area Networks. Part 16: Air Interface for Fixed and Mobile Broadband Wireless Access Systems. Amendment 2: Physical and Medium Access Control Layers for Combined Fixed and Mobile Operation in Licensed Bands. December 2005.

[10] C. R. N. Athaudage, "BER sensitivity of OFDM systems to time synchronization error," *Proc. IEEE ICCS'2002*, vol. 1, pp. 42-46, November 2002.

[11] Y. Mostofi and D. C. Cox, "Mathematical analysis of the impact of timing synchronization errors on the performance of an OFDM system," *IEEE Trans. on Commun.,* vol. 54, no. 2, pp. 226-230, February 2006.

[12] M. Park, K. Ko, H. Yoo, and D. Kong, "Performance analysis of OFDMA uplink systems with symbol timing misalignment," *IEEE Commun. Letters*, vol. 7, no. 8, pp. 376-378, August 2003.

[13] X. Wang, T. T. Tjhung, Y. Wu, and B. Caron, "SER performance evaluation and optimization of OFDM system with residual frequency and timing offsets from imperfect synchronization," *IEEE Trans. on Broadcasting*, vol. 49, no. 2, pp. 170-177, June 2003.